






Article

Thermal Beneficiation of Sra Ouertane (Tunisia) Low-Grade Phosphate Rock

Noureddine Abbes ^{1,*}, Essaid Bilal ², Ludwig Hermann ³, Gerald Steiner ⁴ and Nils Haneklaus ^{4,*}

¹ Groupe Chimique Tunisien, Gabes 6000, Tunisia

² École Nationale Supérieure des Mines de Saint Etienne, 42023 Saint-Etienne, France; bilalessaid@gmail.com

³ Proman Management GmbH, Weingartenstrasse 92, 2214 Auersthal, Austria; l.hermann@proman.pro

⁴ Td Lab Sustainable Mineral Resources, Danube University Krems, Dr.-Karl-Dorrek-Straße 30, 3500 Krems, Austria; gerald.steiner@donau-uni.ac.at

* Correspondence: abbes.nour85@gmail.com (N.A.); nils.haneklaus@donau-uni.ac.at (N.H.)

Received: 7 August 2020; Accepted: 13 October 2020; Published: 22 October 2020



Abstract: Low-grade phosphate rock from Sra Ouertane (Tunisia) was beneficiated using a thermal treatment consisting of calcination, quenching, and disliming. Untreated phosphate rock samples (group 1), calcined phosphate rock samples (group 2), as well as calcined, quenched, and dislimed (group 3) phosphate rock samples, were investigated using inductively-coupled plasma atomic emission spectroscopy (ICP-AES), inductively-coupled plasma mass spectrometry (ICP-MS), thermogravimetric analysis (TGA), and X-ray powder diffraction (XRD). Besides, the particle size distribution of the aforementioned three groups was determined. The proposed thermal treatment successfully increased the P₂O₅ content of the untreated phosphate rock from 20.01 wt% (group 1) to 24.24 wt% (group 2) after calcination and, finally, 27.24 wt% (group 3) after calcination, quenching, and disliming. It was further found that the concentration of relevant accompanying rare earth elements (Ce, La, Nd, Pr, Sm, and Y) was increased and that the concentration of Cd could be significantly reduced from 30 mg/kg to 14 mg/kg with the proposed treatment. The resulting phosphate concentrate showed relatively high concentrations in metal oxides: Σ MgO, Fe₂O₃, Al₂O₃ = 3.63 wt% and silica (9.81 wt%) so that it did not meet the merchant grade specifications of a minimum P₂O₅ content of 30 wt% yet. Removal of these elements could be achieved using additional appropriate separation techniques.

Keywords: thermal beneficiation; calcination; low-grade phosphate rock; Sra Ouertane; Tunisia

1. Introduction

Phosphate rock plays a critical economic role in Tunisia and other countries worldwide. The increasing demand for phosphate rock for fertilizer production and its importance in animal feedstocks, as well as food-grade phosphates and other industrial uses, further solidifies the importance of the phosphate industry in these countries. The demand for phosphate rock is typically fulfilled through phosphate rock mining. The phosphate industry mined nearly 250 million tons of phosphate rock in 2018 [1]. In Tunisia, the phosphate rock industry is of considerable importance to the country's economy. Since the discovery of Tunisian phosphate deposits in the 19th century, phosphate production is controlled and operated by the Gafsa Phosphate Company (CPG, Compagnie des Phosphates de Gafsa, Gafsa, Tunisia). Tunisia has three major phosphate rock deposits: the Northern Basin, the Eastern Basin, and the Gafsa Basin. Figure 1 provides a brief overview of the major phosphate rock deposits in Tunisia.

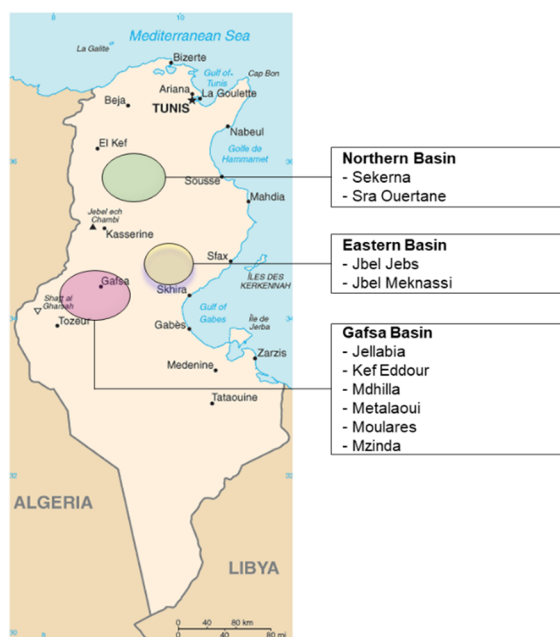


Figure 1. Major phosphate rock deposits in Tunisia.

Currently, more than 90% of the phosphate rock produced in Tunisia is mined from the Gafsa Basin. Tunisia possesses other large phosphate rock deposits with reserves matching those of the Gafsa Basin in quantity but not in quality with regards to the phosphorous (P) content [2]. These deposits are in Sra Ouertane, which is part of the Northern Basin. Up to date, these reserves have not been exploited [3]. With the increased interest in mining of phosphate rock and other monetarily valuable accompanying elements, such as rare earth elements (REEs) and uranium [4–11], presently considered low P-grade deposits are becoming increasingly relevant.

Table 1 provides an overview of the typical P₂O₅, REEs, and uranium concentrations of some mine sites in the Northern-, Eastern-, and Gafsa Basin for which detailed data was made available for this study. The Sra Ouertane low-grade phosphate rock deposit in northern Tunisia can be characterized as a deposit with relatively high uranium and REE content compared to other deposits in Tunisia [12–18].

Table 1. Potential P₂O₅, Uranium, and Rare Earth Element (REE) Concentrations in Some Tunisian Phosphate Rock Deposits [19,20].

| Basin | Deposit | P ₂ O ₅ (wt%) | | | Uranium (mg/kg) | | | Σ REE (mg/kg) | | |
|----------------|-------------|-------------------------------------|------|------|-----------------|-------|------|---------------|------|------|
| | | Min. | Max. | Avg. | Min. | Max. | Avg. | Min. | Max. | Avg. |
| Northern Basin | Sekerna | 19.7 | 23.8 | 21.8 | 36.2 | 55.1 | 45.6 | 750 | 800 | 775 |
| | Sra Ourtane | 21.9 | 26.1 | 24.0 | 73.9 | 112.2 | 93.6 | 401 | 690 | 546 |
| Eastern Basin | Jebel Jebes | 27.9 | 29.5 | 28.7 | 40.8 | 46.7 | 44.1 | 935 | 1020 | 974 |
| Gafsa Basin | Jellabia | 16.4 | 30.3 | 26.0 | 19.9 | 53.7 | 32.7 | 155 | 617 | 432 |
| | Kef Eddour | 25.4 | 28.8 | 26.5 | 23.9 | 41.1 | 31.9 | 171 | 478 | 320 |
| | Metlaoui | 24.1 | 28.3 | 26.4 | 20.9 | 36.2 | 29.9 | 175 | 550 | 326 |
| | Naguess | 23.9 | 29 | 27.2 | 25.4 | 44.2 | 33.6 | 204 | 508 | 345 |

The relatively large amount of impurities found in the Sra Ouertane deposit make beneficiation using flotation technically challenging [21–23]. Calcination is, therefore, considered here for P₂O₅ concentration. Calcination can largely remove carbonates and organic matter from the phosphate rocks. Organic matter can lead to increased use of sulfuric acid for the digestion process that consequently increases overall production costs [24–26]. In this basic technical study, the economics of such a calcination system were not considered yet. The location in Tunisia provides excellent conditions for concentrated solar power, and we hope that phosphate rock from Sra Ouertane could ultimately be

heat treated using solar-powered calcination systems. Reliable cost estimations of the total treatment costs with such solar-powered systems can be provided at a higher technology readiness level.

Currently, approximately 10% of the phosphate rock processed worldwide is calcined [27]. Further depletion of higher grade phosphate rock resources, as well as technical innovations, such as solar-driven calcination of phosphate rocks [28,29], may increase the percentage of phosphate rocks that will be calcined in the future. Previously thermal beneficiation of Tunisian phosphate rock with aluminum silicates [30] and ammonium sulfate [31] has been studied. Furthermore, calcination of Gafsa-Metloui: Jebel Oum El Khacheb deposit [32] and Ras-Dhara deposit [33], as well as M'dhilla [34] phosphate rock, has been investigated, and Jaballi et al. [35] analyzed the thermal behavior of phosphate rocks from the Ypresian phosphate deposit. Besides, Daik et al. [36] and Dabbebi et al. [37] looked into the calcination of phosphate washing waste from the Gafsa-Metloui deposit. The objective of this work was to examine the technical feasibility of a thermal beneficiation path for Sra Ouertane low-grade phosphate rock using calcination, quenching, and disliming.

2. Materials and Methods

The Sra Ouertane deposit consists of three phosphate rock layers (A1, A2, and C). Stratigraphic information of the Sra Ouertane deposit is provided in Figure 2. Samples from layers A1, A2, and C were made available for this study. The usual P_2O_5 concentration of the different layers is as follows: A1 (15–21 wt% P_2O_5), A2 (8–13 wt% P_2O_5), and C (10–13 wt% P_2O_5).

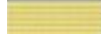








| Lithology | Log | Layer | Thickness (m) | P_2O_5 content (wt%) |
|-----------------------------------|---|-------|---------------|------------------------|
| Ostreas shales, coquinas |  | F | 3 | |
| Nummulitic limestone |  | E | 40 | 1.6 |
| Alternance marly and limestone |  | D | 15 | 4 |
| Coarse phosphate grain |  | C | 10 | 13 |
| Maris |  | B | 1 | 4 |
| Fine calcareous phosphate |  | A2 | 12 | 10 |
| Fine-grained phosphate |  | A1 | 21 | 18 |
| Maris (El Haria formation) |  | M | 100 | |
| White limestone (Abiod formation) |  | Ab3 | 120 | |

Figure 2. Stratigraphic information of the Sra Ouertane deposit in Northern Tunisia [16].

Samples from layers A1, A2, and C of the Sra Ouertane phosphate rock deposit were used for the thermogravimetric analysis (TGA). Later, a detailed sample analysis was performed with samples

from the layer A1. The samples were provided by the National Office of Mines (ONM) of Tunisia and homogenized following the French regulation for the preparation of soil samples (NF X31-101) [38]. The received samples were washed with water, dried at 110 °C overnight, and sieved to give a size fraction less than 250 µm using ASTM (American Society for Testing and Materials) sieves.

Elemental analysis of the samples from layer A1 was conducted using inductively-coupled plasma mass spectrometry (ICP-MS, Perkin Elmer, Woodbridge, ON, Canada) to determine the uranium, thorium, and REE content and inductively-coupled plasma atomic emission spectroscopy (ICP-AES, HORIBA Jobin Yvon, France) for all other constituents. All chemical analyses were conducted with experimental errors below 5%. The particle size distribution was determined using laser diffraction techniques on a Malvern Master Sizer S (Spectris plc, Egham, UK) in the wet mode. X-ray powder diffraction (XRD) analysis was performed using a “Philips MPD1880-PW1710” diffractometer (Philips, Eindhoven, The Netherlands) that uses CuK α radiation ($\lambda = 0.15418$ nm) in the 2–80° interval with a step size of 0.02° and counting time of 20 s/step at room temperature. The identification of the phases was determined using the ICDD-PDF2004 standard database [39].

Of particular relevance for this study was the required calcination temperature and residence time of the phosphate rock that should be processed so that the suitability of solar-driven systems can be determined. Depending on the given phosphate rock, calcination temperatures can vary from as high as 900 °C to as low as 500 °C [40,41]. In this first attempt, the thermal analysis of the samples from layer A1 (9.66 mg sample weight), layer A2 (16.75 mg sample weight), and layer C (12.35 mg sample weight) (particle distribution: 1 mm, 500 µm and 250 µm) was conducted. The characteristic TGA curves for layers A1, A2, and C of the Sra Ouertane phosphate rock are shown in Figure 3. Experiments were conducted at a temperature of up to 800 °C.

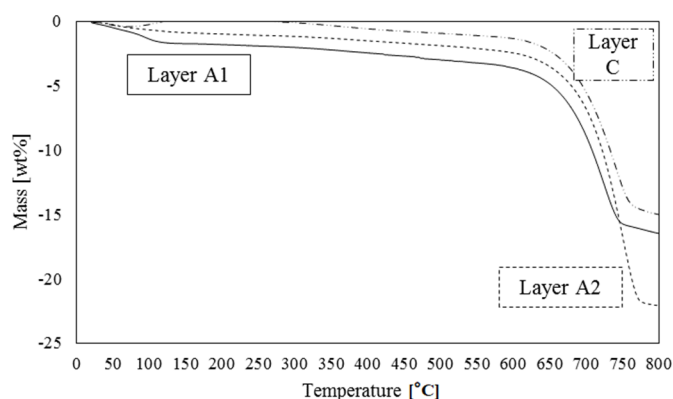
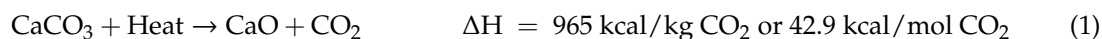


Figure 3. The characteristic thermogravimetric analysis (TGA) curves of the samples from layers A1, A2, and C from Sra Ouertane phosphate rock.

Three peaks, typical of the calcination of phosphate rock, could be identified. The first mass loss at approximately 80 °C corresponded to the removal of adsorbed water. A second weak peak could be identified at approximately 550 °C. Elgharbi et al. [33] attributed this peak to the simultaneous elimination of chemical water in the rock structure and oxidation of organic matter. As most phosphate rocks contain organic matter rich in sulfur, sulfur gas was released. The most pronounced peak was found at 650–750 °C, where carbonate dissociated, and CO₂ was released. Based on the TGA results, the calcination temperature was set to 720 °C. The weight loss at 720 °C was 11.88% (layer A1), 9.72% (layer A2), and 7.90% (layer C), respectively. Best practice experience with conventional kilns in Tunisia recommends a calcination time of 3 h. Thus, calcination experiments were performed at 720 °C for 3 h. It is worth noting that the thermal dissociation of carbonates is an endothermic reaction with a significant energy requirement:



The calcine was further quenched in 5% ammonium nitrate solution with 25% solid content. The calcine was kept in the ammonium nitrate solution for 2 h. In a subsequent disliming process, particles of less than 60 μm were removed using a hydro-cyclone. The preliminary flow sheet of the alternative beneficiation process for Sra Ouertane phosphate rock is provided in Figure 4.

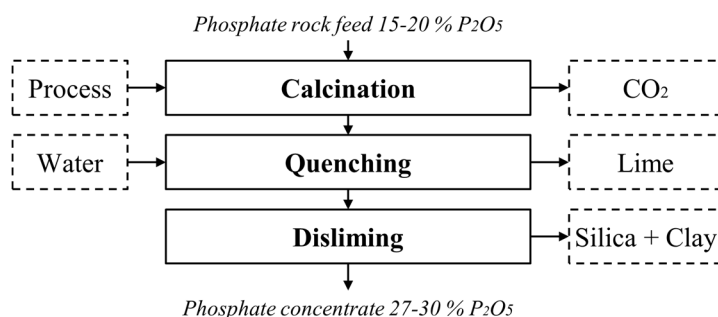


Figure 4. Simplified process flow diagram, describing thermal beneficiation of the Sra Ouertane low-grade phosphate rock by calcination, quenching, and disliming.

3. Results and Discussion

The elemental components relevant for further fertilizer processing of samples from layer A1 are provided in Table 2. The P_2O_5 content of the untreated phosphate rock was successfully increased from 20.01 wt% to 24.24 wt% after calcination. Further treatment consisting of quenching and disliming increased the P_2O_5 content to 27.24 wt%. Merchant grade phosphate rock should show P_2O_5 concentrations of at least 30 wt%. Besides, it is important to mention that the atomic ratio $\text{CaO}/\text{P}_2\text{O}_5 = 1.94$ of the untreated phosphate rock was still higher than the stoichiometric value of francolite with very low carbonate substitution ($\text{CaO}/\text{P}_2\text{O}_5 = 1.65$). Besides, the metal element ratio (MER) of $0.18 = (\text{MgO} + \text{Fe}_2\text{O}_3 + \text{Al}_2\text{O}_3)/\text{P}_2\text{O}_5$ was just slightly below the maximum acceptable value of 0.2.

Table 2. Elemental Analysis of Untreated, Calcined, as Well as Calcined and Treated Sra Ouertane (Layer A1) Phosphate Rock.

| Component | Untreated Phosphate Rock (wt%) | Calcined Phosphate Rock (wt%) | Calcined and Treated Phosphate Rock (wt%) |
|-------------------------|--------------------------------|-------------------------------|---|
| P_2O_5 | 20.01 | 24.24 | 27.24 |
| CaO | 42.93 | 47.01 | 45.65 |
| SO_3 | 1.88 | 2.03 | 2.25 |
| MgO | 1.29 | 1.18 | 0.92 |
| Fe_2O_3 | 1.52 | 1.26 | 1.16 |
| Al_2O_3 | 2.56 | 2.14 | 1.55 |
| SiO_2 | 3.08 | 12.4 | 9.81 |
| CO_2 | 14.78 | 1.95 | 1.95 |
| F | 2.50 | 2.45 | 2.20 |

The calcined and treated phosphate rock, on the other hand, could be associated with the fluorapatite phase. The $\text{CaO}/\text{P}_2\text{O}_5 = 1.68$ was now very close to that of francolite. Besides, the MER of 0.13 was well below the acceptable value of 0.2.

A loss of 39 wt% Al_2O_3 and 30 wt% MgO from untreated phosphate rock to calcined and treated phosphate rock can be observed in Table 2. This loss could be associated with clays that were in a fraction of fewer than 60 microns. It is known that Mg is correlated with CO_3^{2-} apatite, and it could thus be estimated that a portion of MgO was associated with the departure of CO_3^{2-} during calcination. SO_3 increased by 18% in the calcined and treated sample (Table 2). Francolite, the phosphoric mineral of almost all sedimentary phosphorites, has a variable chemical composition that can be represented by $(\text{Ca}, \text{Mg}, \text{Sr}, \text{Na})_{10} (\text{PO}_4, \text{SO}_4, \text{CO}_3)_6 \text{F}_{2-3}$. We hypothesized that a part of the CO_3^{2-} of francolite was

substituted by SO_4^{2-} during calcination in addition to the conventional substitution between PO_4^{3-} and CO_3^{2-} .

Relevant trace element concentrations are provided in Table 3. During the beneficiation process, the cadmium content was significantly reduced from 30 mg/kg to 14 mg/kg. Many countries have legal limits for the cadmium content in fertilizers [42,43] so that reducing the cadmium content early on in the process is a positive side effect of heat treatment of phosphate rock and can be pursued deliberately by controlling the treatment temperature and the oxygen content within the reactor [10]. At temperatures >750 °C, cadmium can be transferred to the gaseous phase and removed through the air pollution control system. Depending on the process parameters and the targeted cadmium removal rate, up to 95% cadmium can be removed from most sedimentary phosphate rock types. Electrostatic precipitation, wet scrubbing, and/or baghouse filters are usually installed for gas cleaning.

Table 3. Relevant Trace Elements in Untreated, Calcined, as Well as Calcined and Treated Sra Ouertane (Layer A1) Phosphate Rock.

| Element | Untreated Phosphate Rock (mg/kg) | Calcined Phosphate Rock (mg/kg) | Calcined and Treated Phosphate Rock (mg/kg) |
|---------|----------------------------------|---------------------------------|---|
| Cd | 30 | 26 | 14 |
| Cr | 160 | 93 | 74 |
| Mn | 67 | 48 | 42 |
| V | 66 | 45 | 43 |
| Zn | 214 | 207 | 142 |
| U | 60 | 68 | 79 |
| Th | 25 | 29 | 34 |

The uranium and thorium contents were increased since volatile constituents in the phosphate rock were driven off. The uranium content at Sra Ouertane reported in the literature (see Table 1) could reach higher concentrations than the uranium concentration that was ultimately measured in the samples here. The uranium concentration measured here would most likely be too low to enable commercially viable uranium recovery [44–47].

Relevant REE concentrations of the Sra Ouertane low-grade phosphate rock are provided in Table 4. The Sra Ouertane phosphate rock deposit showed relatively high REE concentrations by Tunisian [48] and international [9,49] standards, and recovering REEs might be attractive when developing the ore [8,50,51]. During the beneficiation process, all REEs were concentrated as volatile constituents were driven off.

Table 4. Relevant Rare Earth Elements (REEs) in Untreated, Calcined, as Well as Calcined and Treated Sra Ouertane (Layer A1) Phosphate Rock.

| Element | Untreated Phosphate Rock (mg/kg) | Calcined Phosphate Rock (mg/kg) | Calcined and Treated Phosphate Rock (mg/kg) | Crustal Abundance (mg/kg) [52] |
|---------|----------------------------------|---------------------------------|---|--------------------------------|
| Ce | 220 | 240 | 285 | 67 |
| La | 161 | 175 | 192 | 39 |
| Nd | 67 | 76 | 89 | 42 |
| Pr | 29 | 37 | 49 | 9 |
| Sm | 28 | 34 | 47 | 7 |
| Y | 66 | 76 | 88 | 33 |

The particle size distribution was another important parameter for phosphate rock calcination. The particle size of the Sra Ouertane (layer A1) phosphate rock is provided in Figure 5 after sieving with 250 μm ASTM sieves. The particle size distribution of the untreated (Figure 5), calcined (Figure 6), as well as the calcined and treated (Figure 7) phosphate rock, was provided. Calcination slightly increased particle diameters. After calcination, less than 25 vol% of the phosphate rock particles had an equivalent particle diameter below 10 μm . The characteristic peak of particles at 100 μm was present in all stages. It is important to emphasize that the lab-scale experiments conducted here might result in very different particle size distributions than the ones obtained from industrial (rotary kiln) calcination that might, for instance, impose larger friction on the material during processing. The effect of disliming or removal of particles with an equivalent diameter of 60 μm in a hydro-cyclone could best be observed by the difference in particle distribution after calcination and after disliming.

The disliming step conducted on the lab-scale here successfully removed the largest share of small particles that were unwanted in further wet acid processing.

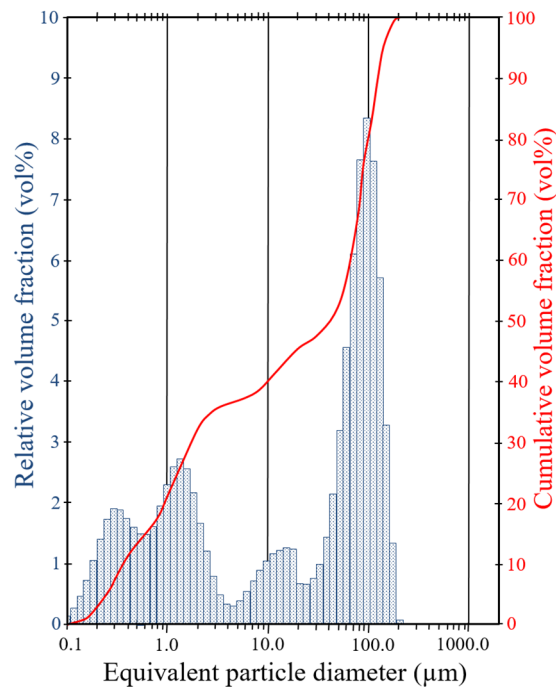


Figure 5. Particle size distribution in vol% of untreated Sra Ouertane (layer A1) phosphate rock.

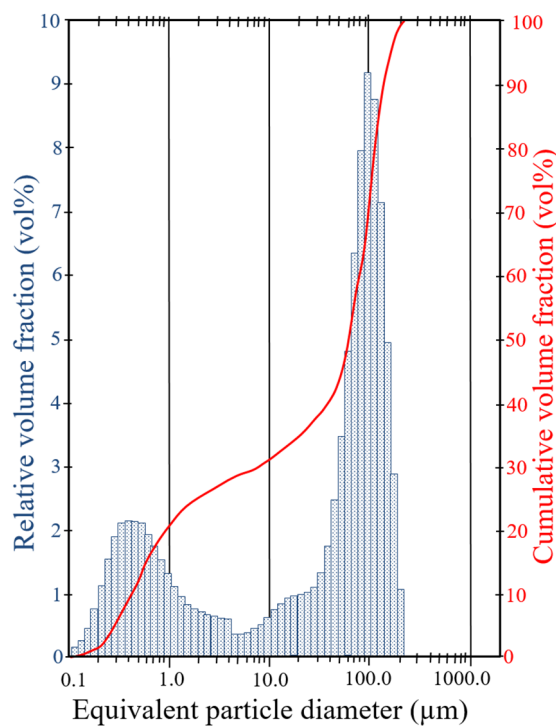


Figure 6. Particle size distribution in vol% of the calcined Sra Ouertane (layer A1) phosphate rock.

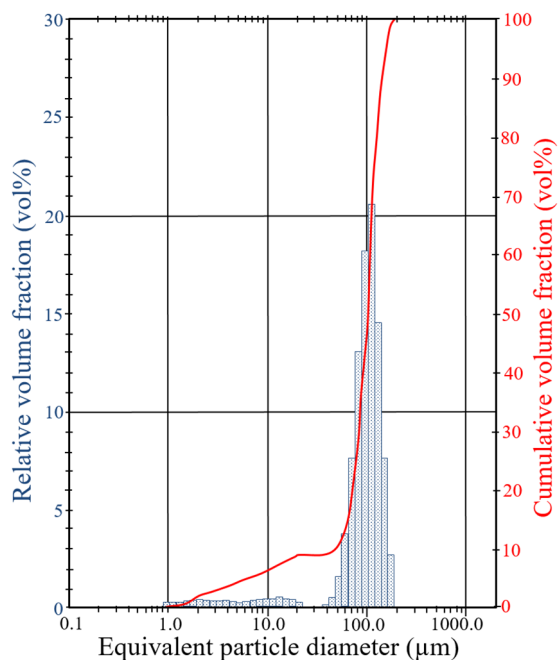


Figure 7. Particle size distribution in vol% of the calcined and treated Sra Ouertane (layer A1) phosphate rock.

XRD analysis was conducted to better understand the effect of the concentration procedure on the phosphate rock. The diffractogram of the XRD analysis was characterized by a number of typical peaks found in other natural sedimentary phosphate rocks (see for instance [32,33,53]) and revealed the presence of the following phases: Fluorapatite ($\text{Ca}_{10}(\text{PO}_4)_6\text{F}_2$), quartz (SiO_2), and carbonates, which are mostly present in the form of calcite (CaCO_3). Figure 8 shows the XRD pattern of the untreated Sra Ouertane phosphate rock.

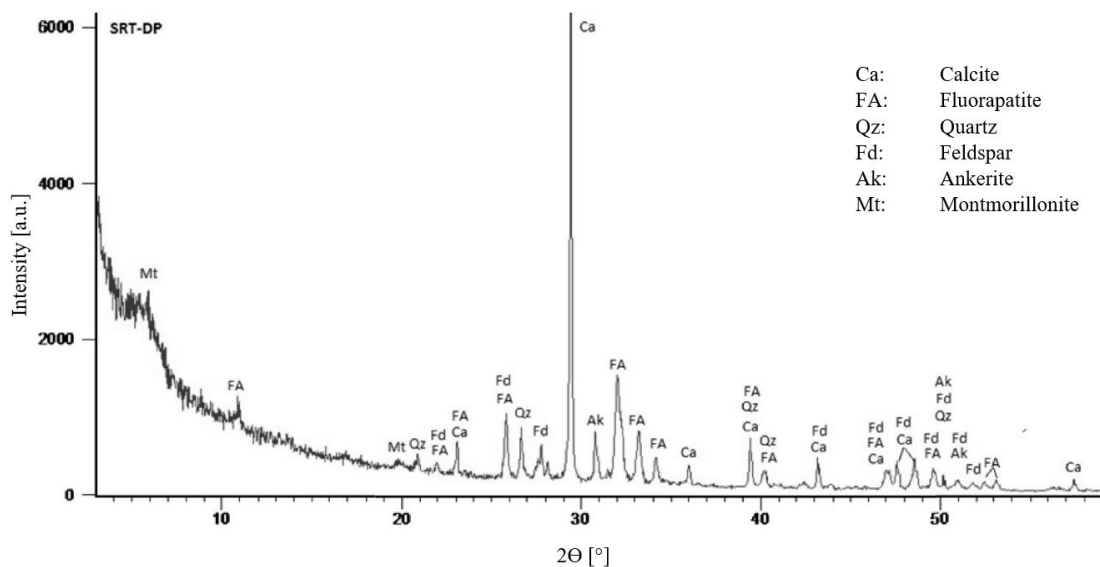


Figure 8. XRD pattern of the untreated Sra Ouertane (layer A1) phosphate rock.

Calcination reduced the CO_2 content of the Sra Ouertane ore significantly. Figure 9 shows the diffractogram of the XRD analysis of the Sra Ouertane phosphate rock after calcination and without the characteristic calcite (CaCO_3) peak that can be observed in Figure 8. Besides, the CaO peaks resulting from carbonate decomposition could be well-identified in the calcined phosphate rock (Figure 9).

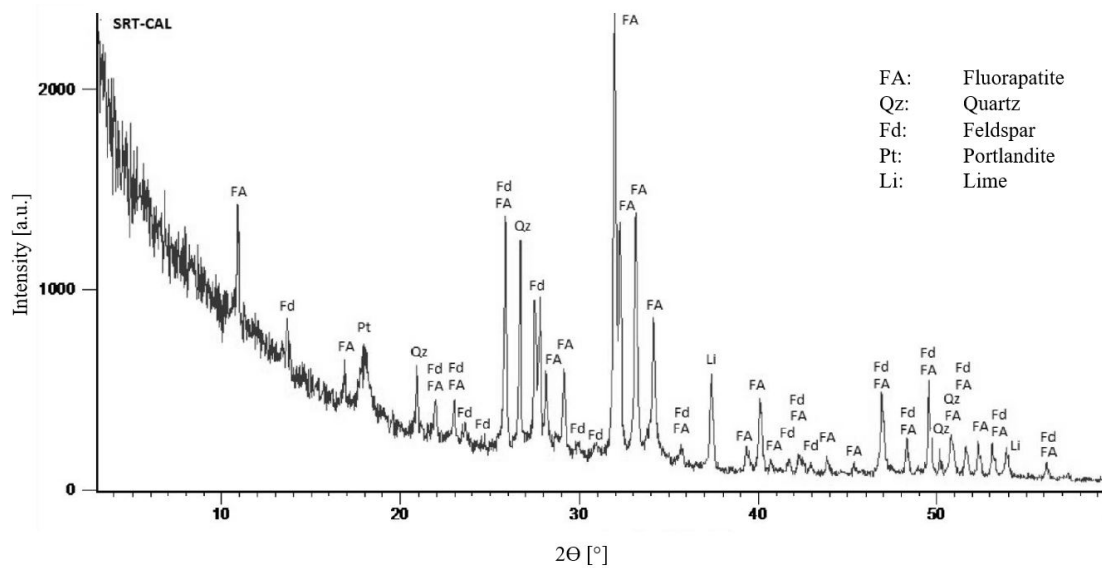


Figure 9. XRD pattern of the calcined Sra Ouertane (layer A1) phosphate rock.

During disliming, smaller particles <60 μm were removed using a hydro cyclone. The XRD pattern of the calcined and treated Sra Ouertane phosphate rock is provided in Figure 10. The absence of peaks related to CaCO₃ and CaO was noticeable. The only remaining mineral species were fluorapatite, quartz, and silicates.

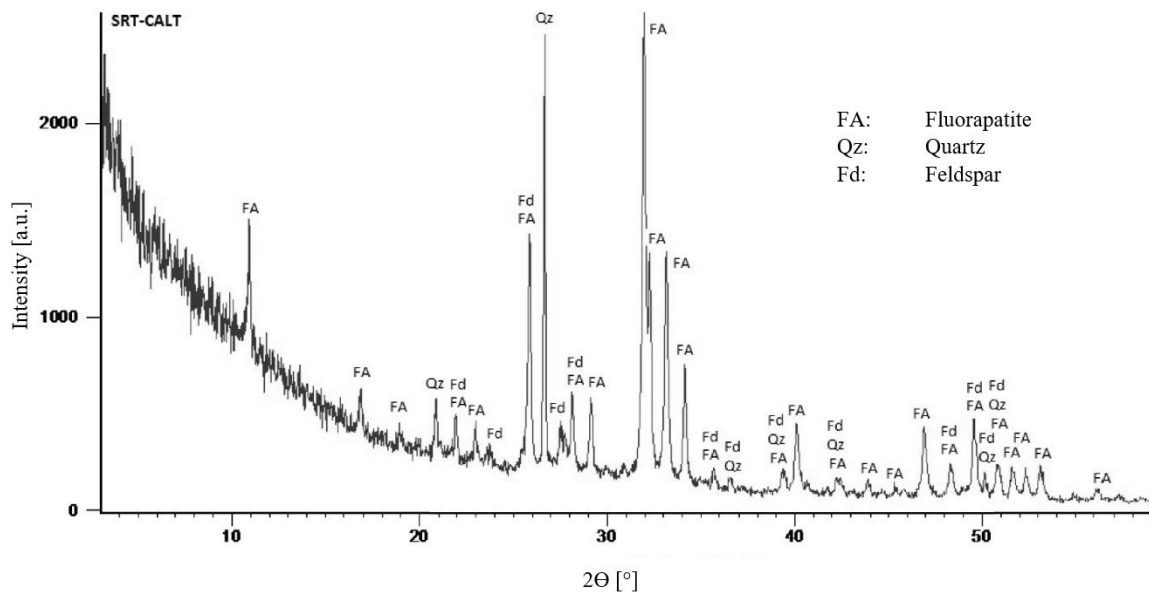


Figure 10. XRD pattern of the calcined and treated Sra Ouertane (layer A1) phosphate rock.

All three XRD patterns are depicted together in Figure 11. Shown is the diffractogram of the untreated phosphate rock (SRT-DP), the calcined phosphate rock (SRT-CAL), as well as the calcined and treated (SRT-CALT) Sra Ouertane phosphate rock (bottom to top). The comparison of the different XRD patterns showed a significant reduction of calcite (CaCO₃) again and thus proved that the process, on a laboratory scale, significantly increased the P₂O₅ content.

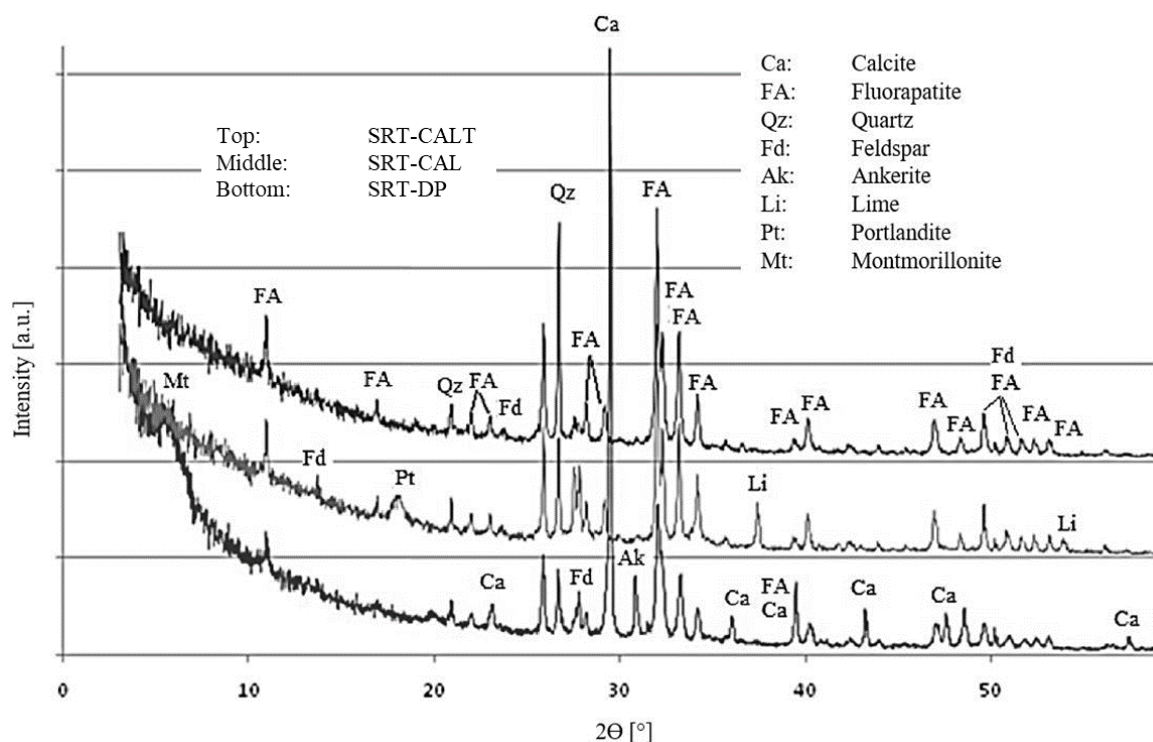


Figure 11. XRD patterns of the calcined and treated (SRT-CALT), calcined (SRT-CAL), as well as untreated (SRT-DP) Sra Ouertane (layer A1) phosphate rock.

4. Conclusions

In total, the P_2O_5 content could be increased from some 20.01 wt% (untreated ore) to 27.24 wt% (calcined and treated ore). To reach merchant grade P_2O_5 concentrations of at least 30 wt%, further processing steps would be required. If, for instance, the relatively high silica content of 9.81 wt% could be reduced to some 2.5 wt%, phosphate concentrate with 30.2 wt% P_2O_5 would result as a final product. It is important to emphasize that even though additional processing steps for further ore concentration are required, the first steps described here are valuable and may help promote the use of Sra Ouertane low-grade phosphate rock ore in a sustainable manner.

Author Contributions: Conceptualization, N.A. and N.H.; methodology, N.A.; writing—original draft preparation, N.H. and N.A.; writing—review and editing, all authors. All authors have read and agreed to the published version of the manuscript.

Funding: This project received funding from the IAEA in Vienna as part of CRP: T11006 [54].

Acknowledgments: The authors are grateful for funding from the IAEA that made this research possible. The views expressed may have not been endorsed by the sponsoring agency. Any remaining errors, omissions, or inconsistencies are the authors' alone.

Conflicts of Interest: The authors declare no conflict of interest.

References

1. USGS. *Phosphate Rock*; United States Geological Survey: Reston, VA, USA, 2015.
2. Boujlel, H.; Daldoul, G.; Tlil, H.; Souissi, R.; Chebbi, N.; Fattah, N.; Souissi, F. The Beneficiation Processes of Low-Grade Sedimentary Phosphates of Tozeur-Nefta Deposit. *Minerals* **2019**, *9*, 2. [[CrossRef](#)]
3. Khleifia, N.; Hannachi, A.; Abbes, N. Studies of uranium recovery from tunisian wet process phosphoric acid. *Int. J. Innov. Appl. Stud.* **2013**, *3*, 1066–1071.
4. Scholz, R.W.; Wellmer, F.-W. Although there is no Physical Short-Term Scarcity of Phosphorus, its Resource Efficiency Should be Improved. *J. Ind. Ecol.* **2018**, *23*, 313–318. [[CrossRef](#)]

5. Geissler, B.; Hermann, L.; Mew, M.C.; Steiner, G. Striving Toward a Circular Economy for Phosphorus: The Role of Phosphate Rock Mining. *Minerals* **2018**, *8*, 395. [[CrossRef](#)]
6. Steiner, G.; Geissler, B.; Haneklaus, N. Making Uranium Recovery from Phosphates Great Again? *Environ. Sci. Technol.* **2020**, *54*, 1287–1289. [[CrossRef](#)]
7. Geissler, B.; Mew, M.C.; Matschullat, J.; Steiner, G. Innovation potential along the phosphorus supply chain: A micro and macro perspective on the mining phase. *Sci. Total Environ.* **2020**, *714*, 136701. [[CrossRef](#)]
8. Emsbo, P.; McLaughlin, P.I.; Breit, G.N.; du Bray, E.A.; Koenig, A.E. Rare earth elements in sedimentary phosphate deposits: Solution to the global REE crisis? *Gondwana Res.* **2015**, *27*, 776–785. [[CrossRef](#)]
9. Chen, M.; Graedel, T.E. The potential for mining trace elements from phosphate rock. *J. Clean. Prod.* **2015**, *91*, 337–346. [[CrossRef](#)]
10. Hermann, L.; Kraus, F.; Hermann, R. Phosphorus processing—Potentials for higher efficiency. *Sustainability* **2018**, *10*, 1482. [[CrossRef](#)]
11. Haneklaus, N.; Sun, Y.; Bol, R.; Lottermoser, B.; Schnug, E. To extract, or not to extract uranium from phosphate rock, that is the question. *Environ. Sci. Technol.* **2017**, *51*, 753–754. [[CrossRef](#)]
12. Da Silva, E.; Mlayah, A.; Gomes, C.; Noronha, F.; Charef, A.; Sequeira, C.; Esteves, V.; Raquel, A.; Marques, F. Heavy elements in the phosphorite from Kalaat Khasba mine (North-western Tunisia): Potential implications on the environment and human health. *J. Hazard. Mater.* **2010**, *182*, 232–245. [[CrossRef](#)] [[PubMed](#)]
13. Tlig, S.; Sassi, A.; Belayouni, H.; Michel, D. Distribution de l'Uranium, du Thorium, du Zirconium, du Hafnium et des Terres Rares (TR) dans des Grains de Phosphates Sédimentaires. *Chem. Geol.* **1987**, *62*, 209–221. [[CrossRef](#)]
14. Sassi, A.B.; Zaier, A.; Joron, J.L.; Treuil, M.; Mao, J.; Bierlein, F.P. Rare earth elements distribution of Tertiary phosphorites in Tunisia. *Miner. Depos. Res. Meet. Glob. Chall.* **2005**, 1161–1164. [[CrossRef](#)]
15. Galfati, I.; Beji Sassi, A.; Zaier, A.; Bouchardon, J.L.; Bilal, E.; Joron, J.L.; Sassi, S. Geochemistry and mineralogy of Paleocene—Eocene Oum El Khecheb phosphorites (Gafsa—Metlaoui Basin) Tunisia. *Geochem. J.* **2010**, *44*, 189–210. [[CrossRef](#)]
16. Gallala, W.; Saïdi, M.; Zayani, K. Characterization and Valorization of Tozeur-Nefta Phosphate Ore Deposit (Southwestern Tunisia). *Procedia Eng.* **2016**, *138*, 8–18. [[CrossRef](#)]
17. Salem, M.; Souissi, R.; Souissi, F.; Abbes, N.; Moutte, J. Phosphoric acid purification sludge: Potential in heavy metals and rare earth elements. *Waste Manag.* **2019**, *83*, 46–56. [[CrossRef](#)]
18. El Zrelli, R.; Rabaoui, L.; Daghbouj, N.; Abda, H.; Castet, S.; Josse, C.; Van Beek, P.; Souhaut, M.; Michel, S.; Bejaoui, N.; et al. Characterization of phosphate rock and phosphogypsum from Gabes phosphate fertilizer factories (SE Tunisia): High mining potential and implications for environmental protection. *Environ. Sci. Pollut. Res.* **2018**, *25*, 14690–14702. [[CrossRef](#)]
19. Abbes, N. Uranium extraction from phosphoric acid: Challenges and opportunities. In Proceedings of the Workshop on “Application of UNFC-2009” for Uranium Resources, Johannesburg, South Africa, 10–14 November 2014.
20. Abbes, N. Processing Low Grade Phosphate Rock from Tunisia using HTGR: Opportunities and challenges. In Proceedings of the CRP-Meeting, Vienna, Austria, 2–5 November 2015.
21. Gharabaghi, M.; Irannajad, M.; Noaparast, M. A review of the beneficiation of calcareous phosphate ores using organic acid leaching. *Hydrometallurgy* **2010**, *103*, 96–107. [[CrossRef](#)]
22. Al-Fariss, T.F.; Ozbelge, H.O.; Abdulrazik, A.M. Flotation of a carbonate rich sedimentary phosphate rock. *Nutr. Cycl. Agroecosyst.* **1991**, *10*, 203–208. [[CrossRef](#)]
23. Guo, F.; Li, J. Separation strategies for Jordanian phosphate rock with siliceous and calcareous gangues. *Int. J. Miner. Process.* **2010**, *97*, 74–78. [[CrossRef](#)]
24. Khaddor, M.; Ziyad, M.; Joffre, J.; Amblès, A. Pyrolysis and characterization of the kerogen from the Moroccan Youssoufia rock phosphate. *Chem. Geol.* **2002**, *186*, 17–30. [[CrossRef](#)]
25. Watti, A.; Alnjar, M.; Hammal, A. Improving the specifications of Syrian raw phosphate by thermal treatment. *Arab. J. Chem.* **2016**, *9*, S637–S642. [[CrossRef](#)]
26. Bezzi, N.; Aïfa, T.; Hamoudi, S.; Merabet, D. Trace Elements of Kef Es Sennoun Natural Phosphate (Djebel Onk, Algeria) and how they Affect the Various Mineralurgic Modes of Treatment. *Procedia Eng.* **2012**, *42*, 1915–1927. [[CrossRef](#)]
27. Abouzeid, A.Z.M. Physical and thermal treatment of phosphate ores—An overview. *Int. J. Miner. Process.* **2008**, *85*, 59–84. [[CrossRef](#)]

28. Haneklaus, N.; Schröders, S.; Zheng, Y.; Allelein, H.-J. Economic evaluation of flameless phosphate rock calcination with concentrated solar power and high temperature reactors. *Energy* **2017**, *140*, 1148–1157. [[CrossRef](#)]
29. Haneklaus, N.; Zheng, Y.; Allelein, H.-J. Stop Smoking—Tube-In-Tube Helical System for Flameless Calcination of Minerals. *Processes* **2017**, *5*, 67. [[CrossRef](#)]
30. Bojinova, D. Thermal treatment of mixtures of Tunisian phosphorite and additives of aluminum silicate. *Thermochim. Acta* **2003**, *404*, 155–162. [[CrossRef](#)]
31. Pelovski, Y.; Petkova, V.; Dombalov, I. Thermal analysis of mechanoactivated mixtures of tunisia phosphorite and ammonium sulfate. *J. Therm. Anal. Calorim.* **2003**, *72*, 967–980. [[CrossRef](#)]
32. Galai, H.; Sliman, F. Mineral characterization of the Oum El Khacheb phosphorites (Gafsa-Metlaoui basin; S Tunisia). *Arab. J. Chem.* **2013**. [[CrossRef](#)]
33. Elgharbi, S.; Horchani-Naifer, K.; Férid, M. Investigation of the structural and mineralogical changes of Tunisian phosphorite during calcinations. *J. Therm. Anal. Calorim.* **2015**, *119*, 265–271. [[CrossRef](#)]
34. Bachouâ, H.; Othmani, M.; Coppel, Y.; Fatteh, N.; Debbabi, M.; Badraoui, B. Structural and thermal investigations of a Tunisian natural phosphate rock. *J. Mater. Environ. Sci.* **2014**, *5*, 1152–1159.
35. Jaballi, F.; Felhi, M.; Khelifi, M.; Fattah, N.; Zayani, K.; Abbes, N.; Elouadi, B.; Tlili, A. Mineralogical and geochemical behavior of heated natural carbonate-apatite of the Ypresian series, Maknassy-Mezzouna basin, central Tunisia. *Carbonates Evaporites* **2019**, *34*, 1689–1702. [[CrossRef](#)]
36. Daik, R.; Lajnef, M.; Amor, S.B.; Ezzaouia, H. Results in Physics Effect of the temperature and the porosity of the gettering process on the removal of heavy metals from Tunisian phosphate rock. *Res. Phys.* **2017**, *7*, 4189–4194.
37. Dabbebi, R.; De Aguiar, J.L.B.; Samet, B.; Baklouti, S. Mineralogical and chemical investigation of Tunisian phosphate washing waste during calcination. *J. Therm. Anal. Calorim.* **2019**, *3*. [[CrossRef](#)]
38. *Qualité du Sol—Préparation d'un Échantillon—NF X 31-101*; Office International de l'Eau (OIEau): Paris, France, 1992.
39. International Centre for Diffraction Data (ICDD). Available online: <https://www.icdd.com/> (accessed on 4 April 2020).
40. Komar Kawatra, S.; Carlson, J.T. *Beneficiation of Phosphate Ore*; Society for Mining, Metallurgy, and Exploration: Englewood, CO, USA, 2013.
41. Tonsuaadu, K.; Gross, K.A.; Pluduma, L.; Veiderma, M. A review on the thermal stability of calcium apatites. *J. Therm. Anal. Calorim.* **2012**, *110*, 647–659. [[CrossRef](#)]
42. Chaney, R.L. *Chapter Two—Food Safety Issues for Mineral and Organic Fertilizers*; Elsevier Science & Technology: Amsterdam, The Netherlands, 2012; Volume 117, ISBN 9780123942784.
43. Ulrich, A.E. Cadmium governance in Europe's phosphate fertilizers: Not so fast? *Sci. Total Environ.* **2019**, *650*, 541–545. [[CrossRef](#)]
44. Tulsidas, H.; Gabriel, S.; Kiegiel, K.; Haneklaus, N. Uranium resources in EU phosphate rock imports. *Resour. Policy* **2019**, *61*, 151–156. [[CrossRef](#)]
45. Haneklaus, N.; Bayok, A.; Fedchenko, V. Phosphate Rocks and Nuclear Proliferation. *Sci. Glob. Secur.* **2017**, *25*, 143–158. [[CrossRef](#)]
46. López, L.; Castro, L.N.; Scasso, R.A.; Grancea, L.; Tulsidas, H.; Haneklaus, N. Uranium supply potential from phosphate rocks for Argentina's nuclear power fleet. *Resour. Policy* **2019**, *62*, 397–404. [[CrossRef](#)]
47. Ye, Y.; Al-Khaledi, N.; Barker, L.; Darwish, M.S.; El Naggar, A.M.A.; El-Yahyaoui, A.; Hussein, A.; Hussein, E.-S.; Shang, D.; Taha, M.; et al. Uranium resources in China's phosphate rocks—Identifying low-hanging fruits Uranium resources in China's phosphate rocks—Identifying low-hanging fruits. *IOP Conf. Ser. Earth Environ. Sci.* **2019**, *227*. [[CrossRef](#)]
48. Garnit, H.; Bouhleb, S.; Barca, D.; Chtara, C. Application of LA-ICP-MS to sedimentary phosphatic particles from Tunisian phosphorite deposits: Insights from trace elements and REE into paleo-depositional environments. *Chemie Erde* **2012**, *72*, 127–139. [[CrossRef](#)]
49. Khater, A.E.M.; Galmed, M.A.; Nasr, M.M.; El-Taher, A. Uranium and rare earth elements in Hazm El-Jalamid phosphate, Saudi Arabia: Concentrations and geochemical patterns comparison. *Environ. Earth Sci.* **2016**, *75*, 1261. [[CrossRef](#)]

50. Wu, S.; Wang, L.; Zhao, L.; Zhang, P.; El-Shall, H.; Moudgil, B.; Huang, X.; Zhang, L. Recovery of rare earth elements from phosphate rock by hydrometallurgical processes—A critical review. *Chem. Eng. J.* **2018**, *335*, 774–800. [[CrossRef](#)]
51. Al Khaledi, N.; Taha, M.; Hussein, A.; Hussein, E.; El Yahyaoui, A.; Haneklaus, N. Direct leaching of rare earth elements and uranium from phosphate rocks. *IOP Conf. Ser. Mater. Sci. Eng.* **2019**, *479*, 012065. [[CrossRef](#)]
52. Jefferson Lab The Periodic Table of Elements. Available online: <https://education.jlab.org/itselemental/index.html> (accessed on 4 August 2020).
53. Koleva, V.; Petkova, V. IR spectroscopic study of high energy activated Tunisian phosphorite. *Vib. Spectrosc.* **2012**, *58*, 125–132. [[CrossRef](#)]
54. Reitsma, F.; Woods, P.; Fairclough, M.; Kim, Y.; Tulsidas, H.; Lopez, L.; Zheng, Y.; Hussein, A.; Brinkmann, G.; Haneklaus, N.; et al. On the sustainability and progress of energy neutral mineral processing. *Sustainability* **2018**, *10*, 235. [[CrossRef](#)]

Publisher’s Note: MDPI stays neutral with regard to jurisdictional claims in published maps and institutional affiliations.



© 2020 by the authors. Licensee MDPI, Basel, Switzerland. This article is an open access article distributed under the terms and conditions of the Creative Commons Attribution (CC BY) license (<http://creativecommons.org/licenses/by/4.0/>).